Electronic Supporting Information

β-Dicyanovinyl Substituted Porphyrinogen: Synthesis, Reversible Sensor for Picric acid among Explosives and Unique Sensor for Cyanide and Fluoride ions by Switching between various Porphyrinoid states

Mandeep K. Chahal and Muniappan Sankar*

Department of Chemistry, Indian Institute of Technology Roorkee, Roorkee-247667, India

Table of Contents

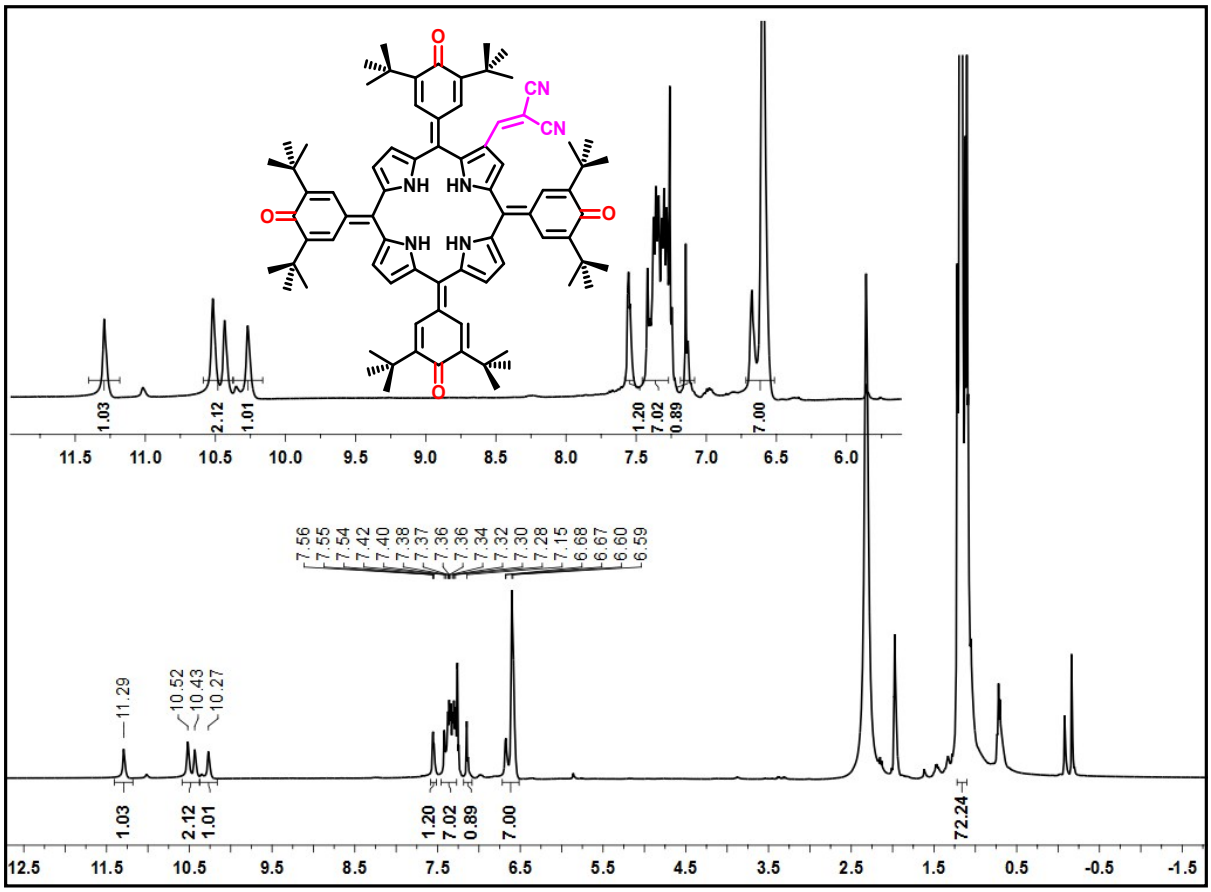

Figure S1. ^{1}H NMR spectrum of OxP-MN (**1**).

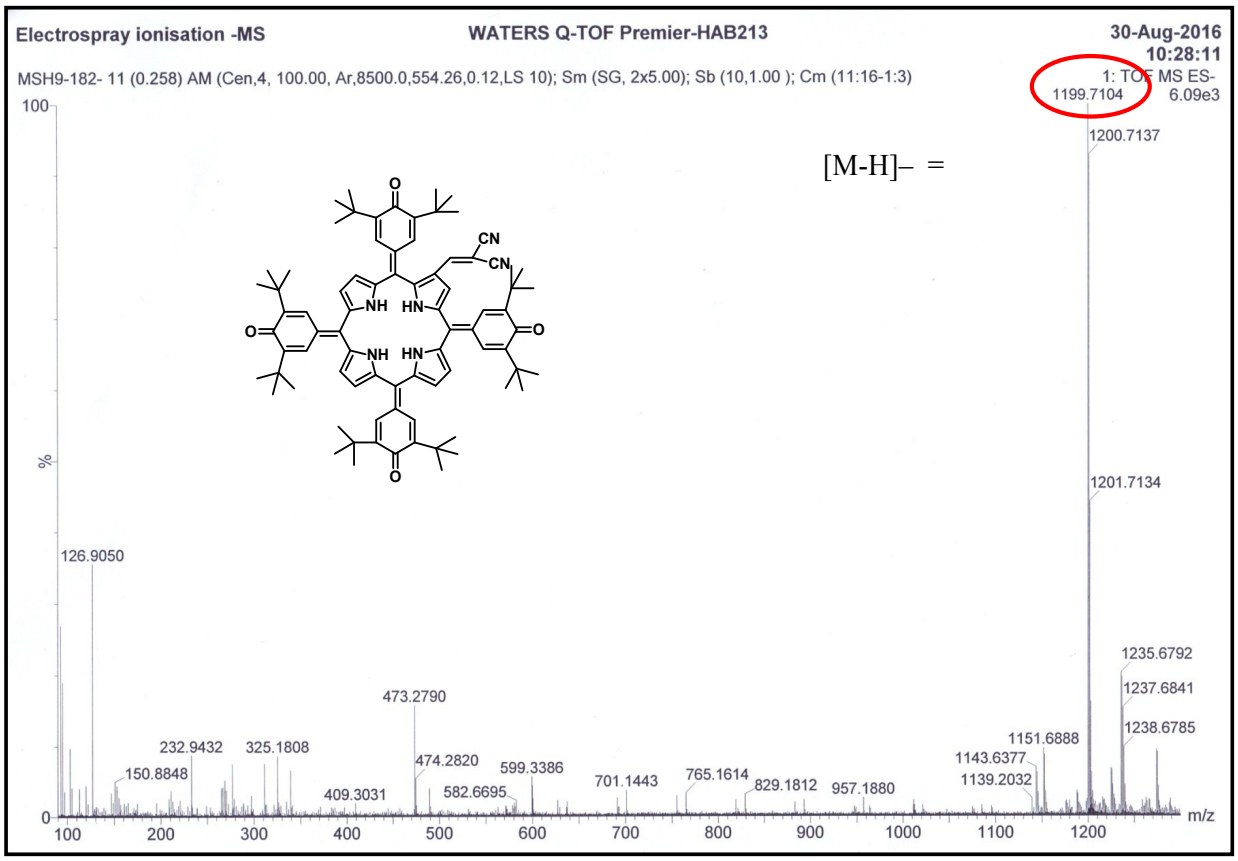

Figure S2. ESI-MS(-) mass spectrum of OxP-MN (**1**).

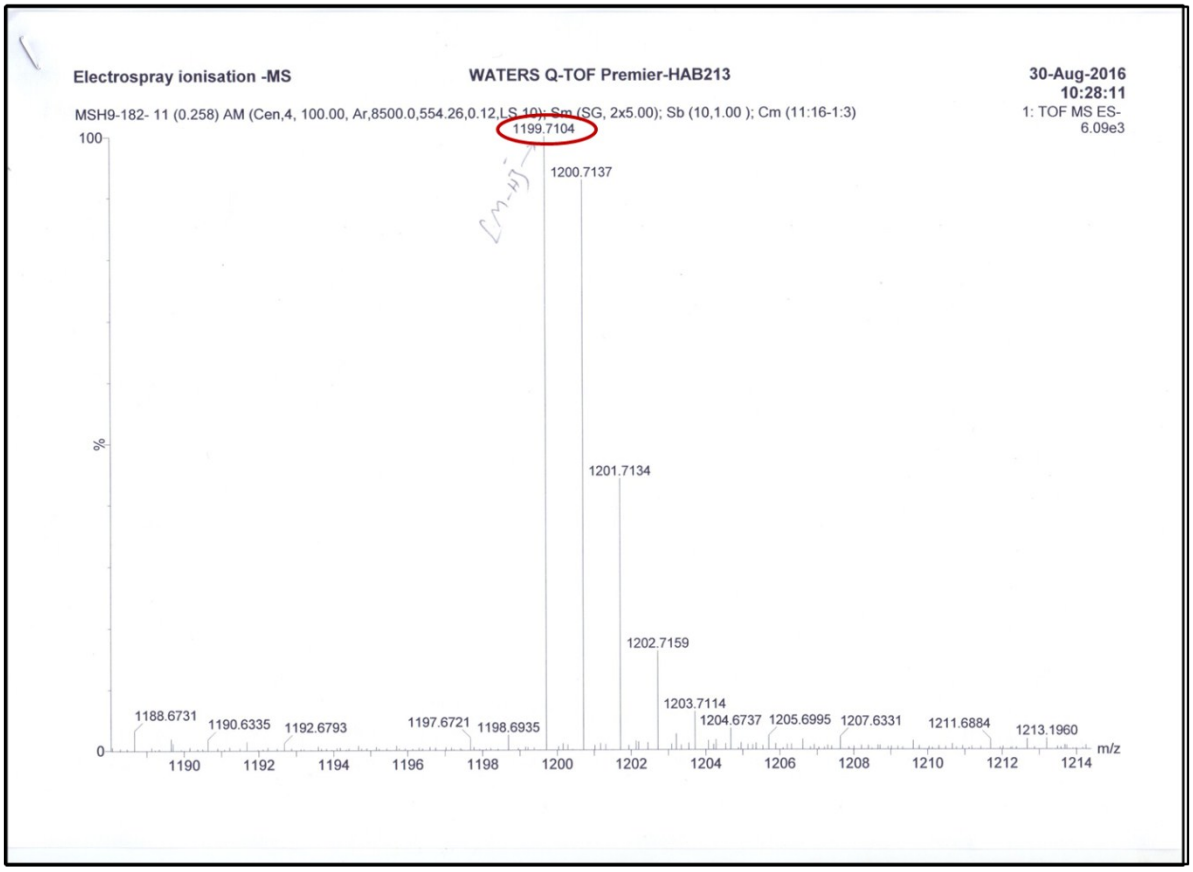

Figure S3. Expanded ESI-MS(-) mass spectrum of OxP-MN (**1**).

Table S1. UV/Vis spectral data of porphyrinogen in CH_2Cl_2 at 298K.

Compound	λ nm
OxP	511
OxP-MN (**1**)	507
β-Br_8OxP	344, 487

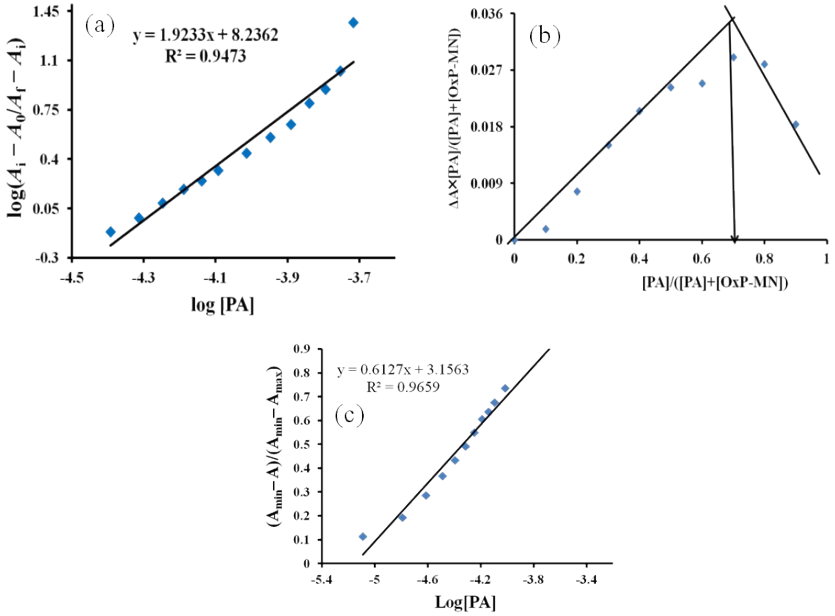

Figure S4. (a) Hill plot for OxP-MN (**1**) and PA system; (b) Job's plot for the complexation of **1** and picric acid (PA): total concentration is constant (1.5 x 10^{-5}M); (c) Absorbance of **1** in CH_2Cl_2, normalized between the minimum absorbance was found at zero equiv of PA and the maximum absorbance.

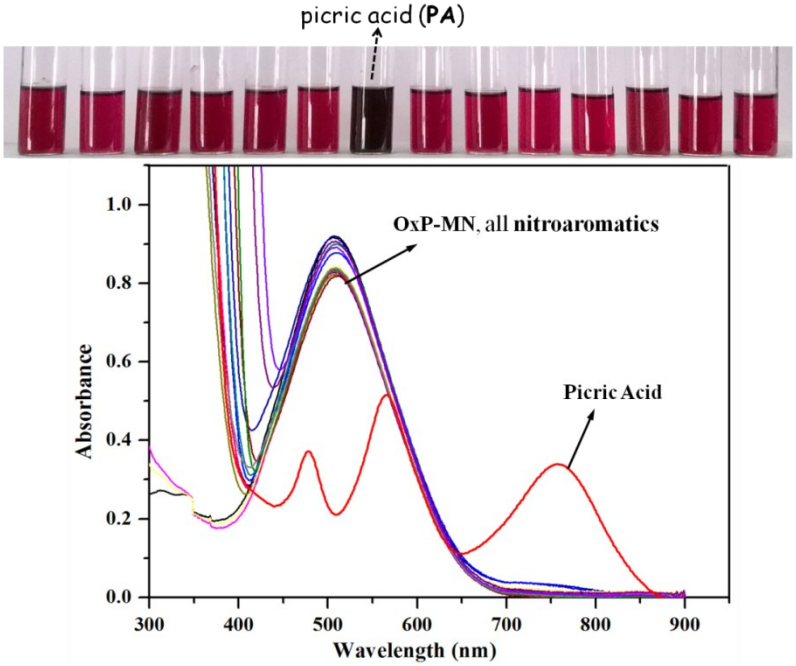

Figure S5. Absorption spectra of OxP-MN in the presence of various NAC's (picric acid (PA)), 2,4-dinitrophenol (2,4-DNP), 4-nitrophenol (4-NP), 4-nitrotoluene (4-NT), nitromethane (NM), nitrobenzene (NB), 1,3-dinitrobenzene (1,3-DNB), 3-nitrotoluene (3-NT), 2,4-dinitrotoluene (2,4-DNT), 4-nitroaniline (4-NA), phenol, 1-iodo-2-nitrobenzene (INB), 2-nitrophenol (2-NP)) in CH_2Cl_2.

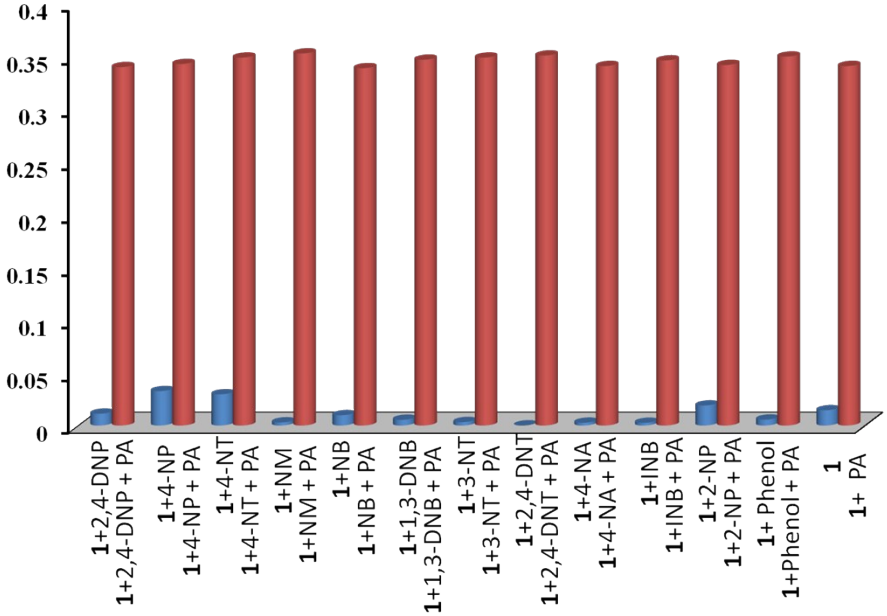

Figure S6. Selectivity of nitroaromatics at a wavelength of 756 nm in a solution having **1** + nitroaromatics (blue bar) and **1** + nitroaromatics + PA (red bar) observed using absorbance spectral studies.

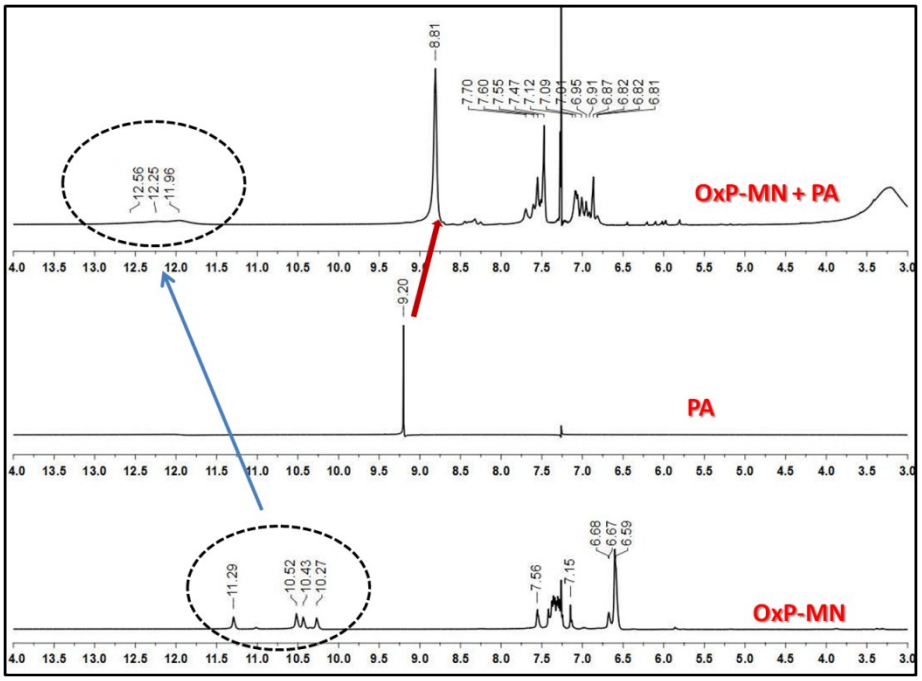

Figure S7. ^{1}H NMR spectra of neat Picric acid (PA) and OxP-MN (**1**) in the absence and presence of picric acid (PA).

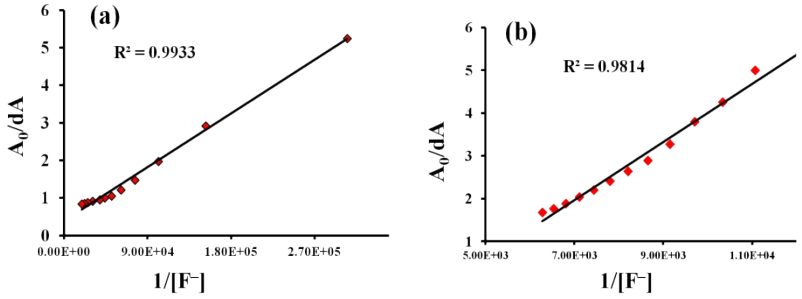

Figure S8. The Benesi-Hildebrand plots constructed for evaluation of binding constants of F^{-} with OxP-MN (**1**).

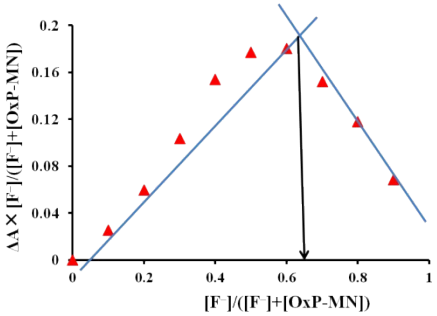

Figure S9. Job's plot for binding of fluoride ions by compound **1** indicating a 2:1 stoichiometry.

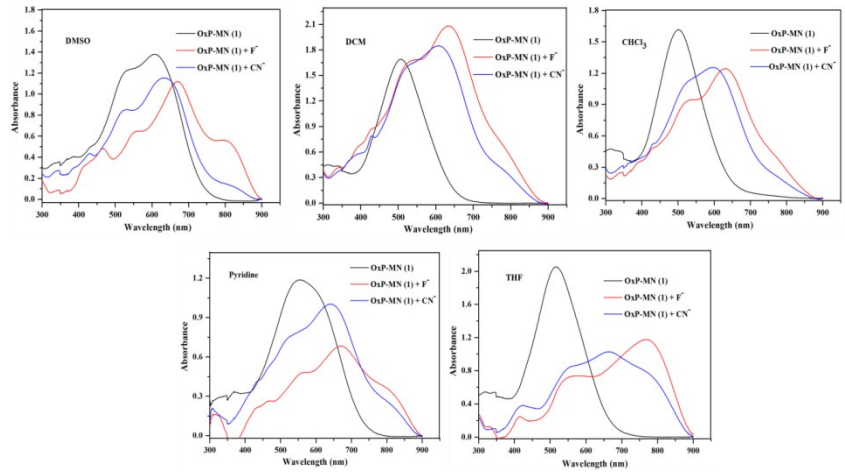

Figure S10. Absorption spectral changes upon addition of F^- and CN^- ions OxP-MN in different solvents.

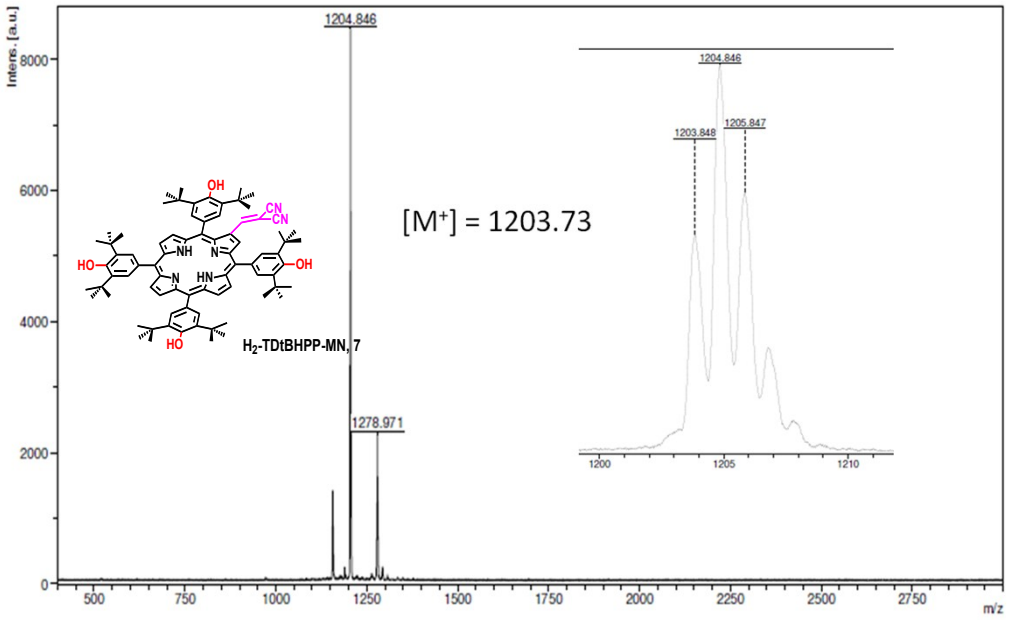

Figure S11. MALDI-TOF mass spectrum of reduced porphyrin (H_2-TDtBHPP-MN, **7**) in case of (OxP-MN•2F^-) using ascorbic acid.

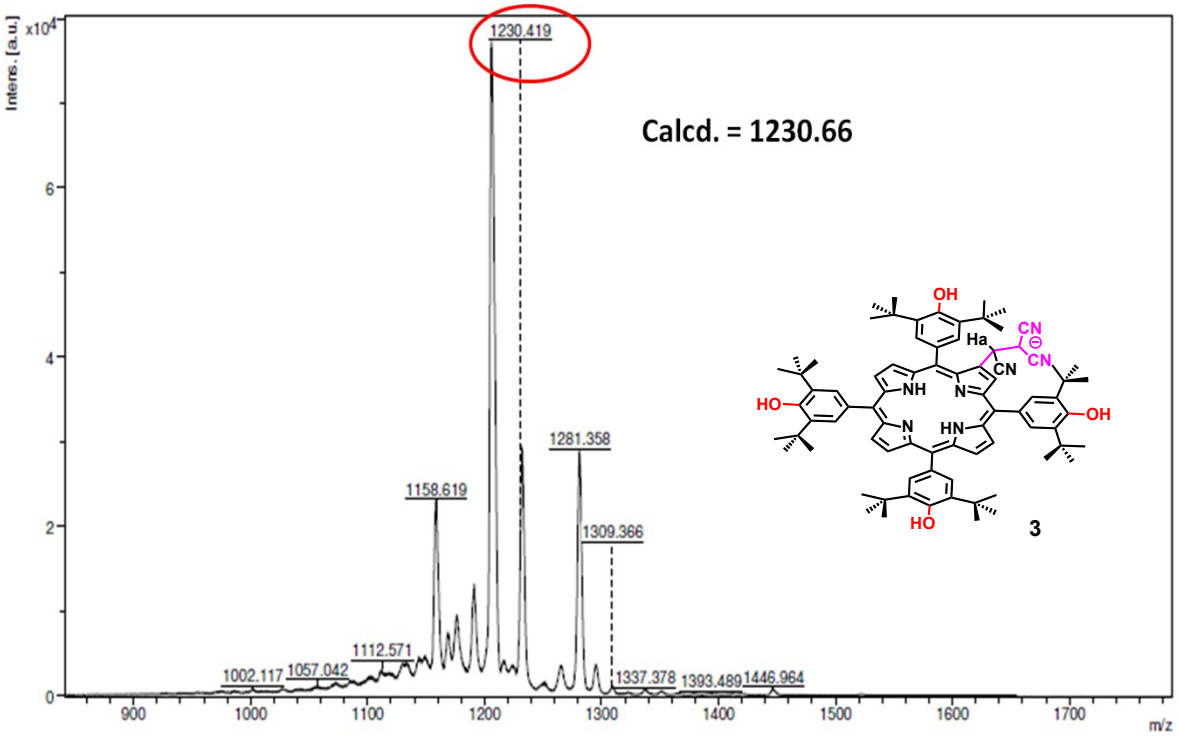

Figure S12. MALDI-TOF mass spectrum of reduced anionic porphyrin (H_2-TDtBHPP-TCE, **3**) derived from cyano adduct of oxoporphyrinogen (**2**) using ascorbic acid.

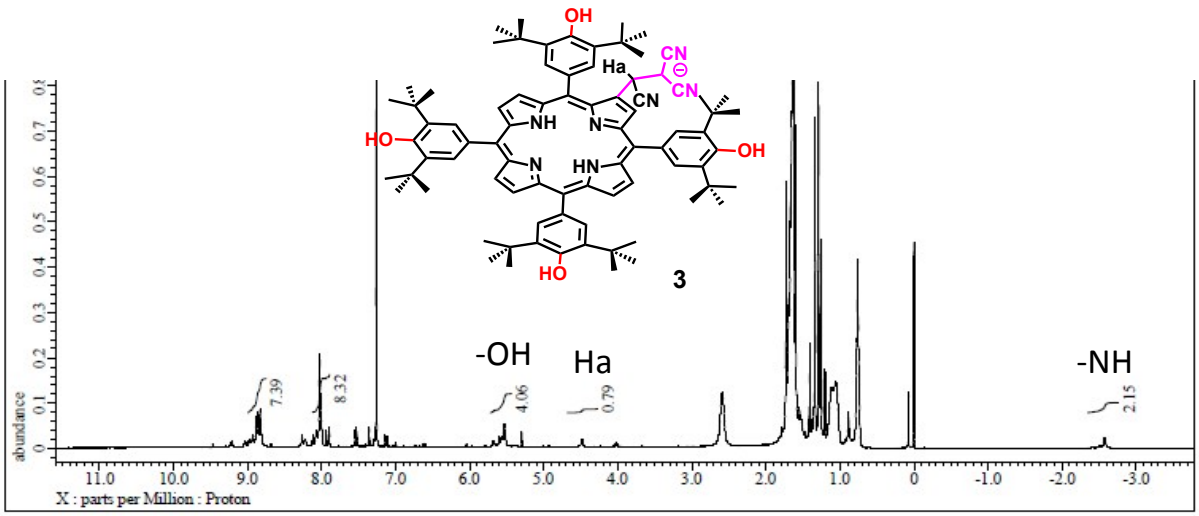

Figure S13. ^{1}H NMR spectrum of reduced anionic porphyrin (H_2-TDtBHPP-TCE, **3**) derived from cyano adduct of oxoporphyrinogen (**2**) using ascorbic acid.

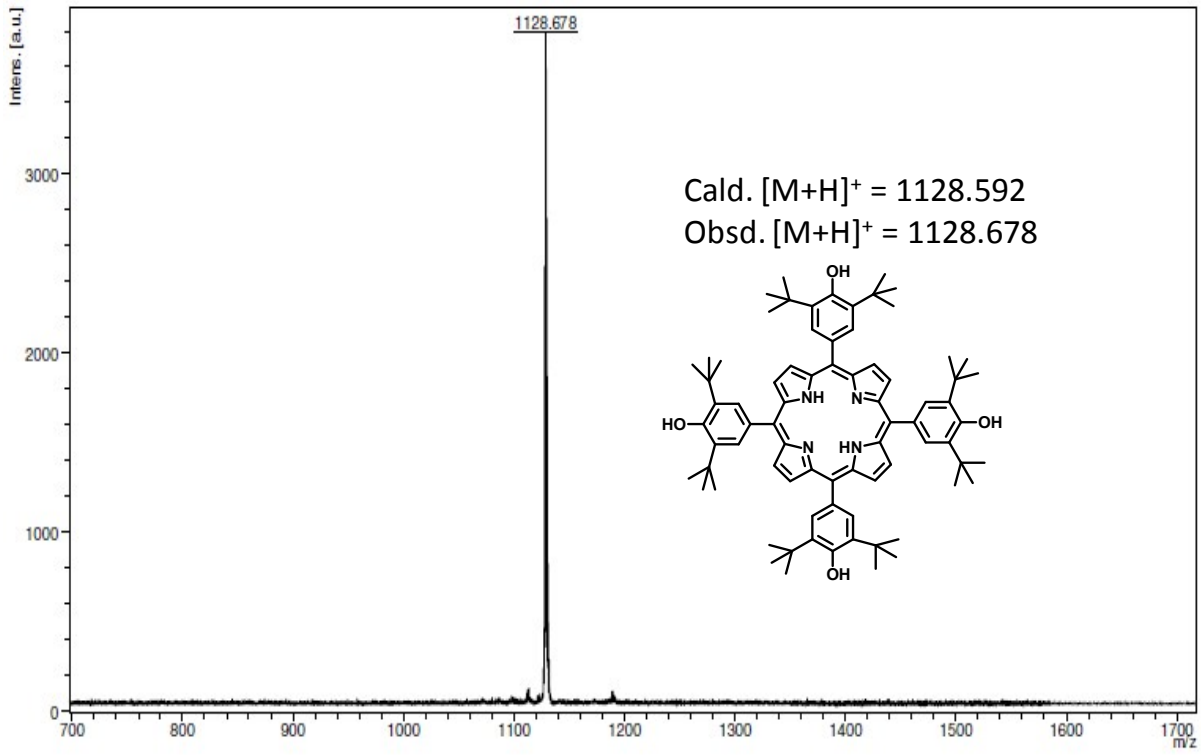

Figure S14. MALDI-TOF mass spectrum of reduced porphyrin (H_2-TDtBHPP) obtained from OxP•2F$^-$ using ascorbic acid as reductant.

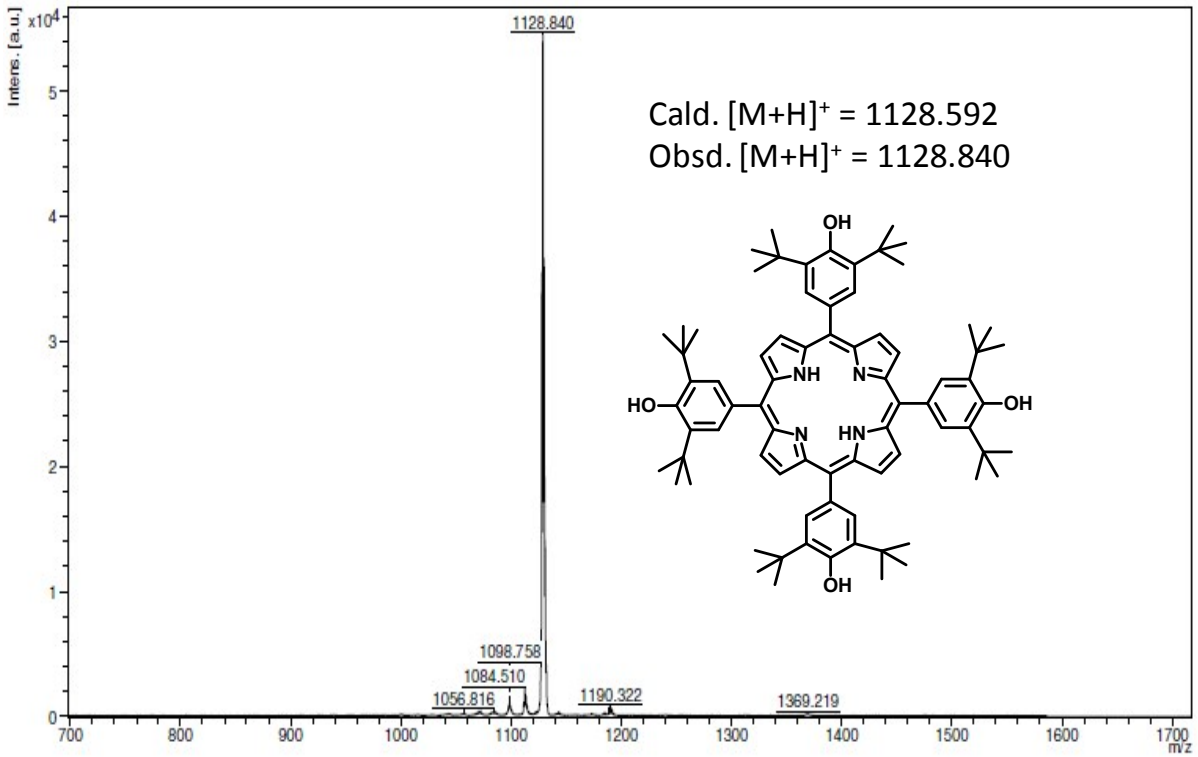

Figure S15. MALDI-TOF mass spectrum of reduced porphyrin (H_2-TDtBHPP) obtained from OxP•2CN$^-$ using ascorbic acid as reductant.

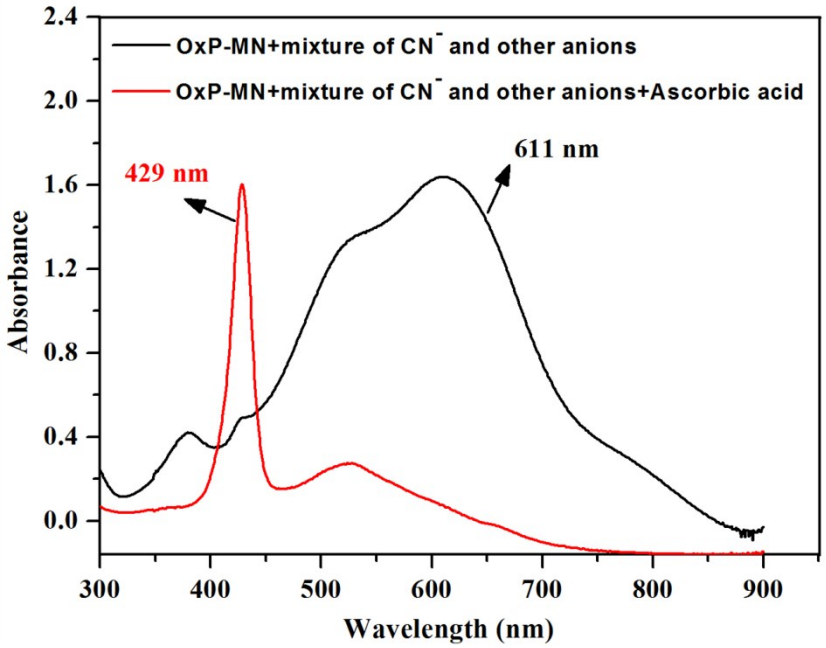

Figure S16. Spectral changes for the competitive recognition of CN^- using a mixture of CN^- and other anions using OxP-MN (**1**).

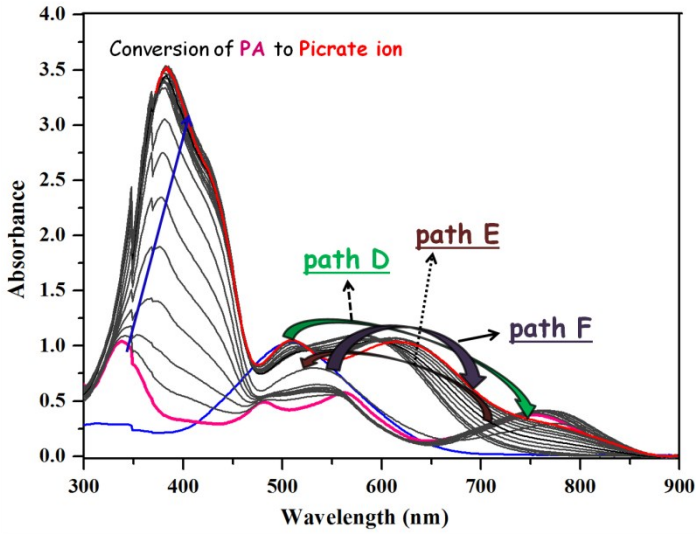

Figure S17. Absorption spectral features of OxP-MN (**1**) on sequential addition of PA and CN^- ions, respectively: path D (porphyrinogen to protonated porphodimethene), path E (protonated porphodimethene to OxP-MN), and path F (OxP-MN to OxP-MN+CN^-•2CN^-).

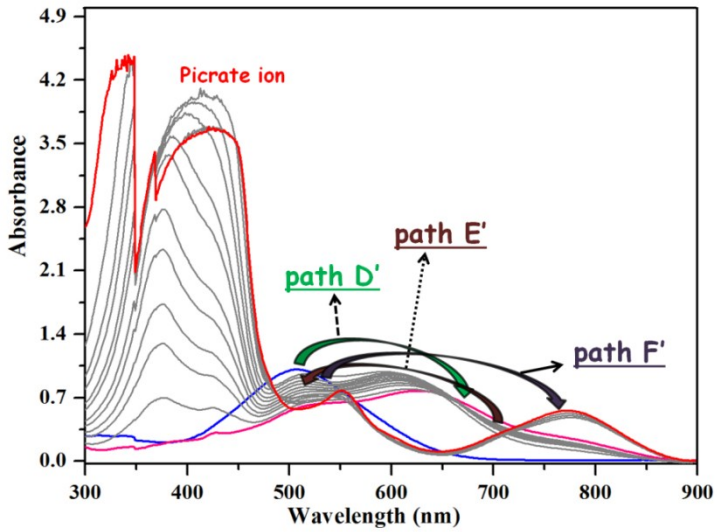

Figure S18. Absorption spectral features of OxP-MN (**1**) on sequential addition of CN^- and PA, respectively: path D' (porphyrinogen to OxP-MN+CN^-•2CN^-), path E' (OxP-MN+CN^- •2CN^- to OxP-MN+CN^-), path F' (OxP-MN+CN^- to anionic protonated porphodimethene).

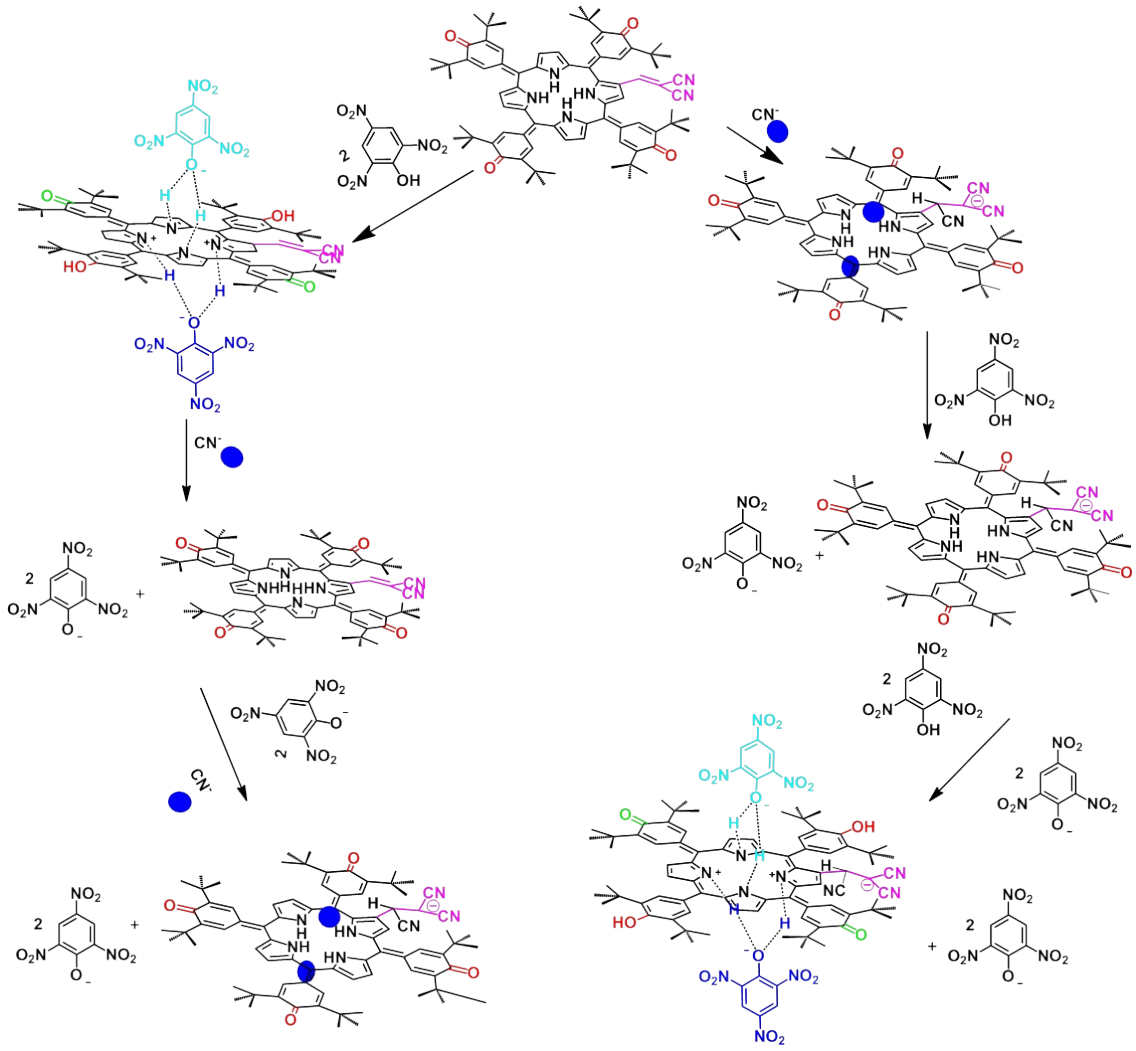

Scheme S1. Response of OxP-MN (**1**) towards CN^- and PA under indicator displacement assay (IDA) without restriction on queue.